The Electronic Spectrum of the C_s-$C_{11}H_3$ Radical

Dongfeng Zhao,[1] **Harold Linnartz,**[2,1] **and Wim Ubachs**[1]

[1]*Institute for Lasers, Life, and Biophotonics, VU University Amsterdam, De Boelelaan 1081, NL 1081 HV Amsterdam, The Netherlands*

[2]*Raymond and Beverly Sackler Laboratory for Astrophysics, Leiden University, P.O. Box 9513, NL 2300 RA Leiden, The Netherlands*

Supplementary Material

Contents:

1. PIB model for an open-shell odd-carbon system

In quantum mechanics, the behavior of a particle in a one-dimensional box is described by three parameters, the principal quantum number (n), the mass of the particle (m), and the box length (L). The quantized energy levels of the particle are expressed as:

$$E(n) = \frac{n^2 h^2}{8mL^2} \tag{S1}$$

where h is the Planck constant.

Hückle molecular orbital theory shows that the π-electrons in conjugated carbon compounds represent a benchmark system for applying the PIB model, by treating the π-electron with mass m as a particle in a box of the conjugated chain with length L, with n the quantum number of the π-orbitals.[20] In a closed-shell **even**-carbon chain system,[41] particularly for the methine chain (polyene chain, -(CH)$_n$-), such as conjugated cyanine dyes, each carbon atom provides one 2p atomic orbital and one π-electron to construct the π-conjugation. The total number of π-electrons is the same as the number of C-atoms in the conjugated system, i.e. N_C (an **even** integer). According to the Pauli exclusion principle, $N_C/2$ π-orbitals will be occupied, i.e.,

$$n_{HOMO} = \frac{N_C}{2}, \qquad n_{LUMO} = \frac{N_C}{2} + 1$$

the optical absorption energy for a $\pi^* \leftarrow \pi$ electronic excitation in closed-shell methine chain (polyene chain, -(CH)$_n$-) systems, such as conjugated cyanine dyes, is described as:[44-45]

$$\begin{aligned} \Delta E = \frac{hc}{\lambda_{abs}} = E_{final} - E_{initial} &= \frac{h^2}{8mL^2}(n_f^2 - n_i^2) \\ &= \frac{h^2}{8mL^2}(N_C + 1) \end{aligned} \tag{S2}$$

In an open-shell **odd**-carbon chain system, the initial and final orbitals upon $\pi \leftarrow \pi$ electronic excitation are the HOMO and singly-occupied molecular orbital (SOMO), repectively. Similarly, the total number of π-electrons is the same as the number of C-atoms, N_C (an **odd** integer). Then, we have

$$n_{HOMO} = \frac{N_C - 1}{2}, \qquad n_{SOMO} = \frac{N_C + 1}{2}$$

The optical absorption energy for an open-shell **odd**-carbon chain system takes the form:

$$\begin{aligned} \Delta E = \frac{hc}{\lambda_{abs}} = E_{final} - E_{initial} &= \frac{h^2}{8mL^2}(n_{SOMO}^2 - n_{HOMO}^2) \\ &= \frac{h^2}{8mL^2} N_C \end{aligned} \qquad \text{（S3）}$$

Using Eq. (S3) and the experimentally observed value of λ_{abs}, the effective box length (L_{eff}) of a odd-carbon chain system can be calculated by

$$L_{eff} = \sqrt{\frac{h \cdot N_C \cdot \lambda_{abs}}{8mc}} \qquad \text{(S4)}$$

The π-conjugation in the bent carbon-chain system is evaluated in terms of this effective box length L_{eff}.

2. Deuterium labeling of a polyhydride by non-equivalent H/D ratio

In a mixed C/H/D plasma, the number of observable D-isotopologues for a specific carrier C_nH_m as well as the statistical production probability of species $C_nH_{m-x}D_x$ ($x \leq m$) are determined by molecular symmetry and unique (i.e., non-interchangeable) hydrogen positions in the geometric carrier structure. Under the assumption that in a plasma jet as used in this experiment, the molecule formation efficiency is barely isotope dependent, the production probability therefore directly provides structural information.

The case of a tri-hydride (C_nH_3) has been discussed in detail in Ref. [28]. In this study focusing on C_{2v}-C_9H_3 and C_{2v}-$C_{11}H_3$,[28] an approximately equivalent H/D ratio was employed in the deuterium-labeling experiment. In this specific case, the statistical production probability ratio of D-isotopologues is approximately the same as their production abundance ratio, i.e., the experimentally determined absorbance ratio. In the case of a non-equivalent H/D ratio, as employed in the deuterium-labeling experiment described here, the observed D-isotopologues abundance ratio has to be rescaled as it also depends on the H/D ratio (1 : x) and the multiplicity of deuteration. For example, the fully hydrogenated and deuterated species of a polyhydride, should have an abundance ratio of about ($1^m : x^m$), where m is the total number of H-atoms in the molecule.

In the present experiment, the absorption intensity ratio of band h_0 and d_0 in Fig. 3c is ~ (1 : 0.50±0.05), and the H/D ratio used in the C/H/D plasma is ~ 1 : 0.8. Because 0.50±0.05 $\simeq 0.8^3 = 0.512$, the total number of hydrogen atoms in the carrier of h_0 can be directly derived as three, i.e., the spectral carrier is a tri-hydride. As discussed in Ref. [28], the observation of eight D-isotoplogues indicates that the three hydrogen atoms are non-interchangeable. Consequently, the relative absorbance (i.e. production abundance) of the eight D-isotopologues can be estimated as:

	H**D**H		HHH		H**DD**		HH**D**		**DD**H		**D**HH		**DDD**		**DHD**
$\simeq$	0.8^{1}	:	0.8^{0}	:	0.8^{2}	:	0.8^{1}	:	0.8^{2}	:	0.8^{1}	:	0.8^{3}	:	0.8^{2}
$\simeq$	0.8	:	1	:	0.64	:	0.8	:	0.64	:	0.8	:	0.51	:	0.64

This is in good agreement with the experimentally determined absorbance ratio shown in Fig. 3c, i.e., ~ 0.8 : 1 : 0.6 : 0.8 : 0.6 : 0.8 : 0.5 : 0.6, and well within a 5% uncertainty in the intensity determination.

3. The lowest-frequency bending vibration in linear or bent carbon chains

The lowest-frequency vibrational mode (C···C···C bending) in a linear or bent carbon chain can be approximated as the bending vibration of a three-center system. In Ref. [46], the normal vibrational modes for both linear and bent tri-atomic molecules have been discussed in detail. The vibrational frequency of the bending vibration, ν, (with Π symmetry) in a linear symmetric YXY molecule is given by

$$4\pi^2\nu^2 = 2\frac{a_{33}}{l^2}\left(\frac{1}{m_Y}+\frac{2}{m_X}\right) \tag{S5}$$

where a_{33} is the bending force constant, l the X-Y bond length, and m_X and m_Y the masses of X and Y, respectively. For the linear $HC_{2n+1}H$ chains, taking Y = C_nH, and X = C, the lowest-frequency vibrational mode, i.e. the HC_n-C-C_nH bending, is described by Eq. (S5). For homologues of the same linear carbon-chain series, m_Y is proportional to l. Because of their similar electronic configuration, the corresponding a_{33} force constant magnitudes are expected to be very close. Thus, it can be found from Eq. (S5) that, the vibrational frequency (ν) of the C···C···C bending mode in linear carbon chains decreases quasi-linearly upon increasing l, which is proportional to the overall chain length. (See DFT-calculated results for $HC_{2n+1}H$ (n = 3–6) in Fig. S1 as an example.)

In Ref. [47], the lowest-frequency bending vibration of 16 linear carbon chains, including polyynes, cyanopolyynes, and dicyanopolyynes, has been studied by DFT calculations. The lowest-frequency bending mode is characterized here in a different way through:

$$\nu = \nu_\infty + ae^{-bn} + ce^{-dn} \tag{S6}$$

where a, b, c, and d are regression coefficients, ν_∞ the limit value of ν for an infinite chain, and n the number of C-atoms. This proposed formula predicts a similar dependence of the C···C···C bending mode, i.e., that ν will decrease upon increasing the number of C-atoms in the chain.

For the bent carbon chains, the lowest-frequency bending vibration (symmetric normal vibration) can be treated as the bending vibration of a non-linear tri-atomic molecule with C_s (XYZ) or C_{2v} (XYX) symmetry. Using the solution for normal vibrational modes of a non-linear tri-atomic molecule as derived in Refs. [46, 48], it can be found that the lowest-frequency C···C···C bending vibration in a bent carbon chain depends on both the overall bent chain length and the bend angle. An analytical approach to quantitatively interpret this case is very complicated. Qualitatively, however, it is concluded that, the larger the overall chain length or the bend angle becomes, the lower the C···C···C bending vibrational energy will be. (See DFT-calculated results for $HC_4CHC_{2n}H$ (n = 1–4) in Fig. S1 as an example.)

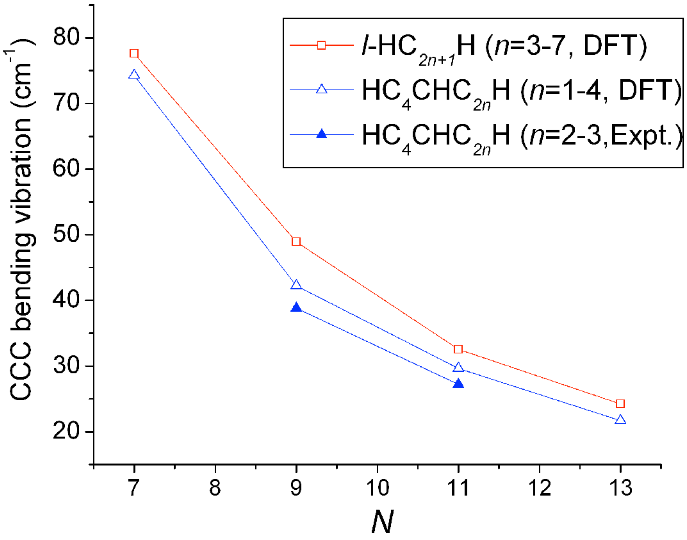

Fig. S1 Calculated and experimentally derived vibrational frequencies of the C···C···C bending mode *vs* total number of C-atoms (N) in linear and bent chains. (□: linear $HC_{2n+1}H$ chains for n = 3–6 and $N = 2n+1$; ▲and Δ: bent $HC_4CHC_{2n}H$ chains for n = 1 – 4 and $N = 2n+5$.)

4. Supporting DFT-calculation results

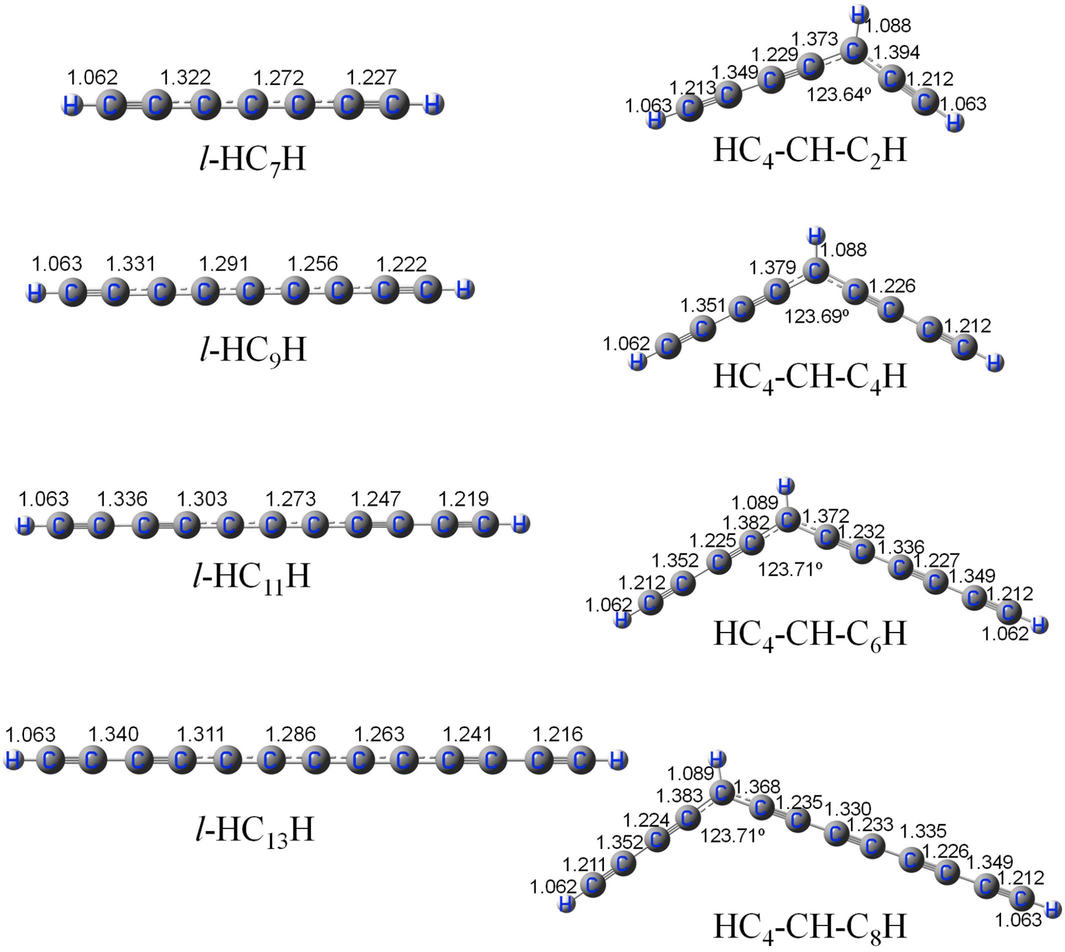

Fig. S2 The molecular structures of bent HC_4-CH-$C_{2n}H$ (n = 1 – 4) and linear $HC_{2n+5}H$ (n = 3 – 6) chains. The bond lengths (in Angstrom) and bend angles are calculated at the DFT-B3LYP/6-311G(d, p) level.

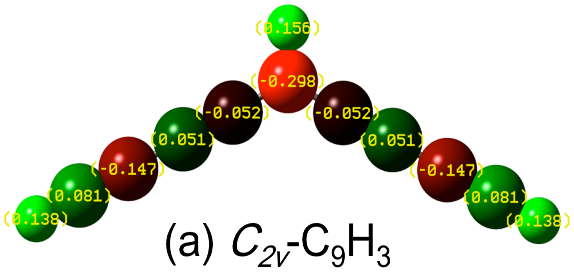

(a) C_{2v}-C_9H_3

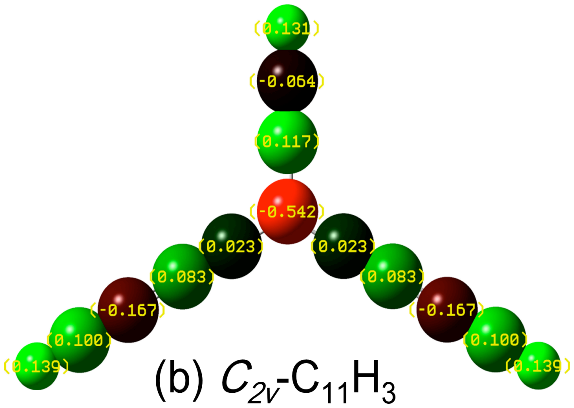

(b) C_{2v}-$C_{11}H_3$

Fig. S3 DFT calculated Mulliken charge distribution of C_{2v}-C_9H_3 and C_{2v}-C11H3.

Table S1 Ground state vibrational frequencies (in cm^{-1}) of l-HC$_{2n+1}$H (n = 3 – 6) and HC$_4$-CH-C$_{2n}$H (n = 1 – 4) calculated at B3LYP/6-311G(d, p) level

Species	Vibrational frequency and symmetry
l-HC$_7$H	3465.9 (σ_g), 3463.4 (σ_u), 2048.8 (σ_g), 2015.2 (σ_u), 1683.6 (σ_g), 1660.4 (σ_u), 1081.0 (σ_u), 561.4 (σ_g); 602.1 (π_u), 531.2 (π_g), 519.5 (π_u), 466.5 (π_g), 393.7 (π_u), 197.3 (π_g), 80.2 (π_u).
l-HC$_9$H	3467.0 (σ_g), 3465.8 (σ_u), 2097.1 (σ_u), 2063.6 (σ_g), 2030.2 (σ_g), 1741.8 (σ_u), 1559.0 (σ_u), 1251.7 (σ_g), 859.9 (σ_u), 442.8 (σ_g); 828.2 (π_u), 583.6 (π_g), 570.0 (π_u), 547.1 (π_g), 466.5 (π_u), 396.4 (π_g), 236.0 (π_u), 133.3 (π_g), 50.5 (π_u).
l-HC$_{11}$H	3468.6 (σ_g), 3467.8 (σ_u), 2138.8 (σ_u), 2105.1 (σ_g), 2043.4 (σ_g), 2036.2 (σ_u), 1768.1 (σ_g), 1464.5 (σ_u), 1354.1 (σ_u), 1047.3 (σ_g), 714.0 (σ_u), 365.5 (σ_g); 609.9 (π_g), 597.2 (π_u), 587.1 (π_g), 545.0 (π_u), 468.3 (π_u), 458.4 (π_g), 390.9 (π_u), 257.2 (π_g), 171.6 (π_u), 92.1 (π_g), 33.6 (π_u).
l-HC$_{13}$H	3469.0 (σ_g), 3468.4 (σ_u), 2152.9 (σ_g), 2150.8 (σ_u), 2102.9 (σ_u), 2044.9 (σ_g), 1992.4 (σ_g), 1786.6 (σ_u), 1425.7 (σ_g), 1367.0 (σ_u), 1171.8, 899.7 (σ_g), 609.7 (σ_u), 310.9 (σ_g); 672.6 (π_g), 619.5 (π_u), 608.2 (π_g), 593.5 (π_u), 516.2 (π_g), 495.5 (π_u), 453.1 (π_u), 391.6 (π_g), 275.6 (π_u), 201.2 (π_g), 128.1 (π_u), 67.4 (π_g), 24.5 (π_u).
HC$_4$-CH-C$_2$H	3472.6 (a'), 3469.7 (a'), 3130.0 (a'), 2173.6 (a'), 2117.6 (a'), 2043.2 (a'), 1417.7 (a'), 1242.6 (a'), 1036.2 (a'), 784.6 (a'), 675.3 (a'), 639.7 (a'), , 546.6 (a'), 502.2 (a'), 344.0 (a'), 196.0 (a'), 76.7 (a'); 699.6 (a''), 603.4 (a'') 573.8 (a''), 509.6 (a''), 378.4 (a''), 352.3 (a''), 142.4 (a'').
HC$_4$-CH-C$_4$H	3474.1 (a_1), 3119.3 (a_1), 2220.7 (a_1), 2119.8 (a_1), 1225.0 (a_1), 774.6 (a_1), 644.3 (a_1), 535.1 (a_1), 452.6 (a_1), , 214.2 (a_1), 43.4 (a_1); 3473.5 (b_2), 2147.9 (b_2), 2051.3 (b_2), 1434.1 (b_2), 1241.5 (b_2), 785.6 (b_2), 644.2 (b_2), 527.2 (b_2), 338.4 (b_2), 135.4 (b_2); 615.5 (a_2), 522.1 (a_2), 374.8 (a_2), 130.8 (a_2); 712.6 (b_1), 615.7 (b_1), 510.6 (b_1), 353.6 (b_1), 154.8 (b_1).
HC$_4$-CH-C$_6$H	3473.1 (a'), 3472.5 (a'), 3114.4 (a'), 2225.7 (a'), 2203.9 (a'), 2138.2 (a'), 2114.7 (a'), 2003.5 (a'), 1466.1 (a'), 1321.5 (a'), 1234.8 (a'), 1013.9 (a'), 776.1 (a'), 648.6 (a'), 645.5 (a'), 640.7 (a'), 621.1 (a'), 526.2 (a'), 521.4 (a'), 493.1 (a'), 408.8 (a'), 340.4 (a'), 243.0 (a'), 164.5 (a'), 88.5 (a'), 30.6 (a'); 720.5 (a''), 636.9 (a''), 620.7 (a''), 610.9 (a''), 494.2 (a''), 377.0 (a''), 355.9 (a''), 204.2 (a''), 144.2 (a''), 76.1 (a'').
HC$_4$-CH-C$_8$H	3473.5 (a'), 3473.1 (a'), 3112.9 (a'), 2251.1 (a'), 2209.0 (a'), 2180.4 (a'), 2126.7 (a'), 2090.8 (a'), 1960.9 (a'), 1498.2 (a'), 1366.9 (a'), 1234.2 (a'), 1156.8 (a'), 851.1 (a'), 774.7 (a'), 647.3 (a'), 642.4 (a'), 575.1 (a'), 554.2 (a'), 530.8 (a'), 514.9 (a'), 456.4 (a'), 365.9 (a'), 339.4 (a'), 262.1 (a'), 181.4 (a'), 128.1 (a'), 60.0 (a'), 22.4 (a'); 724.9 (a''), 638.3 (a''), 624.7 (a''), 551.8 (a''), 525.9 (a''), 517.3 (a''), 459.1 (a''), 374.6 (a''), 355.8 (a''), 238.3 (a''), 148.1 (a''),125.4 (a''), 47.0 (a''),

Table S2 Ground state vibrational frequencies (in cm^{-1}) of (partially) deuterated C_s-C$_{11}$H$_3$ calculated at B3LYP/6-311G(d, p) level

Species	Vibrational frequency and symmetry
HC$_4$-C**D**-C$_6$**H**	3473.1 (a'), 3472.5 (a'), 2292.7 (a'), 2224.7 (a'), 2203.8 (a'), 2138.2 (a'), 2113.7 (a'), 2003.4 (a'), 1451.7 (a'), 1289.1 (a'), 1060.9 (a'), 914.8 (a'), 752.1 (a'), 646.2 (a'), 644.9 (a'), 634.8 (a'), 617.0 (a'), 525.6 (a'), 491.4 (a'), 407.5 (a'), 336.2 (a'), 242.4 (a'), 163.8 (a'), 88.2 (a'), 30.5 (a'); 642.5 (a''), 631.9 (a''), 620.7 (a''), 608.8 (a''), 519.3 (a''), 488.1 (a''), 376.8 (a''), 332.9 (a''), 197.3 (a''), 137.6 (a''), 74.4 (a'').
HC$_4$-C**D**-C$_6$**D**	3472.6 (a'), 2684.9 (a'), 2292.6 (a'), 2213.3 (a'), 2190.3 (a'), 2130.3 (a'), 2051.3 (a'), 1974.8 (a'), 1448.4 (a'), 1285.5 (a'), 1056.5 (a'), 911.4 (a'), 752.1 (a'), 646.0 (a'), 636.6 (a'), 616.7 (a'), 525.4 (a'), 511.2 (a'), 477.0 (a'), 404.5 (a'), 333.6 (a'), 237.7 (a'), 161.9 (a'), 86.3 (a'), 30.0 (a'); 639.7 (a''), 620.7 (a''), 615.7 (a''), 519.7 (a''), 502.8 (a''), 473.8 (a''), 372.5 (a''), 330.7 (a''), 192.0 (a''), 137.6 (a''), 72.5 (a'').
HC$_4$-C**H**-C$_6$**D**	3472.6 (a'), 3114.3 (a'), 2684.9 (a'), 2213.8 (a'), 2190.9 (a'), 2131.0 (a'), 2051.5 (a'), 1974.9 (a'), 1463.5 (a'), 1317.1 (a'), 1234.7 (a'), 1006.5 (a'), 776.1 (a'), 646.7 (a'), 642.5 (a'), 622.7 (a'), 526.0 (a'), 511.7 (a'), 478.5 (a'), 405.7 (a'), 337.9 (a'), 238.2 (a'), 162.6 (a'), 86.6 (a'), 30.1 (a'); 720.5 (a''), 620.7 (a''), 521.5 (a''), 505.6 (a''), 477.6 (a''), 372.6 (a''), 353.9 (a''), 198.9 (a''), 143.9 (a''), 74.1 (a'').
DC$_4$-C**D**-C$_6$**H**	3473.0 (a'), 2682.6 (a'), 2292.6 (a'), 2221.9 (a'), 2196.9 (a'), 2123.9 (a'), 2023.4 (a'), 1995.7 (a'), 1450.1 (a'), 1282.9 (a'), 1056.9 (a'), 914.5 (a'), 747.4 (a'), 644.7 (a'), 633.6 (a'), 616.5 (a'), 529.8 (a'), 498.1 (a'), 491.2 (a'), 404.6 (a'), 332.8 (a'), 239.8 (a'), 159.7 (a'), 87.2 (a'), 29.9 (a'); 642.5 (a''), 631.9 (a''), 608.8 (a''), 522.7 (a''), 492.6 (a''), 477.1 (a''), 373.0 (a''), 327.2 (a''), 197.3 (a''), 132.7 (a''), 74.3 (a'').
DC$_4$-C**H**-C$_6$**H**	3473.0 (a'), 3114.3 (a'), 2682.6 (a'), 2223.2 (a'), 2196.9 (a'), 2124.3 (a'), 2023.9 (a'), 1995.8 (a'), 1464.5 (a'), 1319.6 (a'), 1228.6 (a'), 1012.7 (a'), 770.1 (a'), 646.9 (a'), 640.4 (a'), 621.0 (a'), 530.3 (a'), 498.4 (a'), 492.9 (a'), 405.9 (a'), 336.9 (a'), 240.5 (a'), 160.3 (a'), 87.5 (a'), 30.0 (a'); 720.5 (a''), 636.9 (a''), 610.9 (a''), 524.5 (a''), 495.5 (a''), 481.1 (a''), 374.4 (a''), 348.6 (a''), 204.2 (a''), 139.0 (a''), 75.9 (a'').
DC$_4$-C**D**-C$_6$**D**	2684.9 (a'), 2682.6 (a'), 2292.5 (a'), 2203.8 (a'), 2189.8 (a'), 2058.6 (a'), 2012.2 (a'), 1973.6 (a'), 1446.6 (a'), 1279.2 (a'), 1052.5 (a'), 911.1 (a'), 747.4 (a'), 635.6 (a'), 615.8 (a'), 529.7 (a'), 511.3 (a'), 497.8 (a'), 476.9 (a'), 401.6 (a'), 330.2 (a'), 235.0 (a'), 157.8 (a'), 85.3 (a'), 29.5 (a'); 639.7 (a''), 615.7 (a''), 522.8 (a''), 504.1 (a''), 483.5 (a''), 470.6 (a''), 368.3 (a''), 325.5 (a''), 192.0 (a''), 132.6 (a''), 72.3 (a'').
DC$_4$-C**H**-C$_6$**D**	3114.3 (a'), 2684.9 (a'), 2682.6 (a'), 2204.9 (a'), 2190.2 (a'), 2058.7 (a'), 2012.7 (a'), 1973.7 (a'), 1461.9 (a'), 1315.3 (a'), 1228.1 (a'), 1005.3 (a'), 770.1 (a'), 641.7 (a'), 622.5 (a'), 530.1 (a'), 511.7 (a'), 498.1 (a'), 478.4 (a'), 402.8 (a'), 334.4 (a'), 235.6 (a'), 158.5 (a'), 85.6 (a'), 29.6 (a'); 720.5 (a''), 620.0 (a''), 524.5 (a''), 506.1 (a''), 483.6 (a''), 476.0 (a''), 368.9 (a''), 347.7 (a''), 198.8 (a''), 138.7 (a''), 73.9 (a'').

Table S3 TD-DFT (B3LYP/6-311G(2d, p)) predicted vertical excitation energies of HC_4-CH-$C_{2n}H$ ($n = 1 - 4$)

Molecules	Transitions	Excitation energy	Oscillator strength
HC_4-CH-C_2H	$1^2A'' - X^2A''$	2.82 eV	0.063
HC_4-CH-C_4H	$1^2A_2 - X^2B_1$	2.49 eV	0.085
HC_4-CH-C_6H	$1^2A'' - X^2A''$	2.20 eV	0.078
HC_4-CH-C_8H	$1^2A'' - X^2A''$	1.95 eV	0.057

5. Comparisons of the H/D isotopic shifts

Table **S4** Experimentally determined H/D isotopic shifts (in cm^{-1})

Molecules	Di-deuteration		Mono-deuteration		
l-HC_7H[a]	+125.2		+62.2	HC_3-**C-C_3-H/D**	
l-HC_9H[a]	+77.9		+38.8	HC_4-**C-C_4-H/D**	
l-$HC_{11}H$[a]	+50.6		+25.4	HC_5-**C-C_5-H/D**	
l-$HC_{13}H$[a]	+34.9		+17.3	HC_6-**C-C_6-H/D**	
C_{2v}-C_9H_3[b]	+70.6	Δ^{I+III}	+34.9	HC_4-**HC-C_4-H/D**	$\Delta^{I/III}$
C_s-$C_{11}H_3$[c]	+44.5	Δ^{I+III}	+13.6	HC_4-**HC-C_6-H/D**	Δ^{I}
			+30.6	HC_6-**HC-C_4-H/D**	Δ^{III}

[a] Ref. [19]. [b] Ref. [28]. [c] This work.

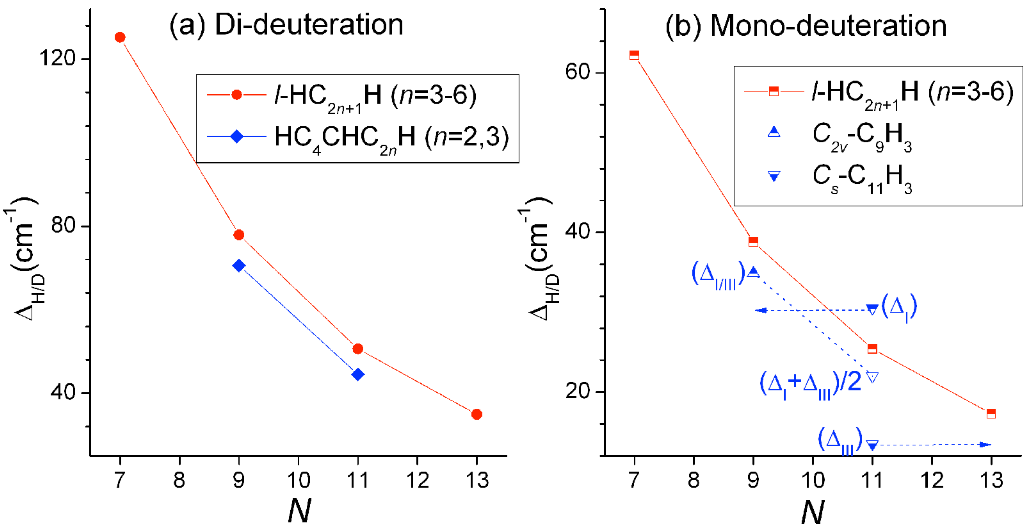

Fig. S4 Comparisons of the H/D isotopic shifts between the electronic origin band transitions of linear and bent HC···C(H)···CH chains by mono- and di-deuteration.

6. References

[31] Gaussian 03, Revision B.04, M. J. Frisch, G. W. Trucks, H. B. Schlegel, G. E. Scuseria, M. A. Robb, J. R. Cheeseman, J. A. Montgomery, Jr., T. Vreven, K. N. Kudin, J. C. Burant, J. M. Millam, S. S. Iyengar, J. Tomasi, V. Barone, B. Mennucci, M. Cossi, G. Scalmani, N. Rega, G. A. Petersson, H. Nakatsuji, M. Hada, M. Ehara, K. Toyota, R. Fukuda, J. Hasegawa, M. Ishida, T. Nakajima, Y. Honda, O. Kitao, H. Nakai, M. Klene, X. Li, J. E. Knox, H. P. Hratchian, J. B. Cross, C. Adamo, J. Jaramillo, R. Gomperts, R. E. Stratmann, O. Yazyev, A. J. Austin, R. Cammi, C. Pomelli, J. W. Ochterski, P. Y. Ayala, K. Morokuma, G. A. Voth, P. Salvador, J. J. Dannenberg, V. G. Zakrzewski, S. Dapprich, A. D. Daniels, M. C. Strain, O. Farkas, D. K. Malick, A. D. Rabuck, K. Raghavachari, J. B. Foresman, J. V. Ortiz, Q. Cui, A. G. Baboul, S. Clifford, J. Cioslowski, B. B. Stefanov, G. Liu, A. Liashenko, P. Piskorz, I. Komaromi, R. L. Martin, D. J. Fox, T. Keith, M. A. Al-Laham, C. Y. Peng, A. Nanayakkara, M. Challacombe, P. M. W. Gill, B. Johnson, W. Chen, M. W. Wong, C. Gonzalez, and J. A. Pople, Gaussian, Inc., Pittsburgh PA, 2003.

[45] G. Calzaferri, Chimia **41**, 248 (1987).

[46] G. Herzberg, *Molecular Spectra and Molecular Structure II. Infrared and Raman Spectra of Polyatomic Molecules Reprint Edition*, Krieger Publishing company, Malabar, Florida; p131–200 (1991).

[47] A. Scemana, P. Chaquin, M. C. Gazeau, and Y. Benilan, J. Phys. Chem. A **106**, 3828 (2002).

[48] P. C. Cross, J. H. Van Vleck, J. Chem. Phys. **1**, 350 (1933).